

# Finite Element Analysis on Piezoelectric Ring Transformer

Hing Leung Li, Jun Hui Hu, *Member, IEEE*, and Helen Lai Wah Chan

**Abstract**—The use of a piezoelectric ring as transformer is reported and studied in this paper. By using a concentric electrode pattern, a ring-shaped transformer can be designed to operate at its high order extensional modes. Lead zirconate titanate (PZT) ceramic rings with 12.7-mm outer diameter, 5.1-mm inner diameter and 1.2-mm thickness were used to fabricate the prototypes. Three-dimensional (3-D) finite element models are built to study and analyze the vibration characteristics of the piezoelectric transformers (PTs) using higher order modes ( $>3$ ). The resonant frequencies, mean coupling effect, mode shapes, and other open-circuit characteristics are simulated and compared with experimental measurements. Prototypes of PTs using mode order three and four were fabricated and characterized. Good agreement can be obtained between experimental results and finite element model (FEM) simulations. The dimensions for the PTs using higher order symmetric extensional modes are optimized by FEM. To avoid mode coupling with the thickness mode, the ideal ring thickness has to be less than or equal to 0.6 mm. The ring PT offers advantages of simple structure and small size. It has a good potential in making low cost PT for low-voltage applications.

## I. INTRODUCTION

THE idea of a piezoelectric transformer (PT) was first implemented by Rosen in 1956 [1]. It used the coupling effect between electrical and mechanical energy of piezoelectric materials. A sinusoidal signal is used to excite mechanical vibrations by the inverse piezoelectric effect via the driver section. Due to the direct piezoelectric effect, an output voltage can be induced in the generator part. The PT offers many advantages over the conventional electromagnetic transformer such as high power-to-volume ratio, electromagnetic field immunity, and nonflammable. Due to the demand on miniaturization of power supplying systems of electrical equipment, the study of PTs has become a very active research area in engineering. In the literature [2], [3], many PTs have been proposed and a few of them found practical applications. Apart from switching power supply system, a Rosen-type PT has been adopted in cold cathode fluorescent lamp inverters for liquid-crystal displays [2]. The PT with multilayer structure to provide

high-output power may be used in various kinds of power supply units [3]. Recently, PTs of ring or disk shapes have been proposed and investigated [4]–[9]. Their main advantages are simple structure and small size. In comparing with the structure of a ring and a disk, the PZT ring offers higher electromechanical coupling in the radial direction [8]. The high-electromechanical coupling implies that a ring structure is more efficient in converting mechanical energy to electrical energy, and vice versa, which is essential for a high performance PT. Therefore, ring-shaped PTs are very suitable in making low-cost PTs for low-voltage applications.

In a previous study [6], [9], a ring transformer operated at the third symmetric extensional mode was proposed and developed. Different from all the conventional PTs, the ring PT proposed only required a single poling process and a proper electrode pattern. The PT was fabricated by a PZT ring by dividing one of the electrodes into two concentric circular regions. The third symmetric extensional mode was used as the operation mode. Prototypes were fabricated, and a maximum efficiency and power density of 92.3% and 14.3 W/m<sup>3</sup>, respectively, could be achieved. With a similar approach, PTs using higher-order modes also could be designed by using proper electrode patterns. Because of the mode coupling effect and the complexity of vibration modes at high frequency, the conventional lumped-equivalent circuit method may not accurately predict the dynamic behaviors of the PTs. In this study, a commercial finite-element code (ANSYS, ANSYS, Inc., Houston, TX) was used as a computational tool to analyze and study the ring piezoelectric transformer. The purpose of using FEM is to predict the actual physical behaviors of the PT without going through the expensive prototyping processes. It can help to manipulate and analyze the effects of various design variables. In this study, different electrode patterns were designed to excite the higher-order extensional modes of a PZT ring. Three-dimensional FEM were built to study the dynamic behavior at its resonance. Laser vibrometer measurement was performed to verify that the required extensional modes were excited. Good agreements were obtained between laser measurement and the FEM simulation. The performances of PTs using various vibration modes have been studied. The performance of the PT was evaluated by the mean coupling factor of input and output sections ( $k_m$ ). The open-circuit characteristics were simulated and compared with measurement results. The dimensions of the ring were optimized to avoid mode coupling effect.

Manuscript received June 29, 2003; accepted June 14, 2004. The authors would like to acknowledge the supports by the Center for Smart Materials of the Hong Kong Polytechnic University and the Innovation and Technology Fund (ITF UIM/29) of the HKSAR Government.

The authors are with the Department of Applied Physics and Materials Research Center, The Hong Kong Polytechnic University, Hungghom, Kowloon, Hong Kong, China (e-mail: marchy@netvigator.com).

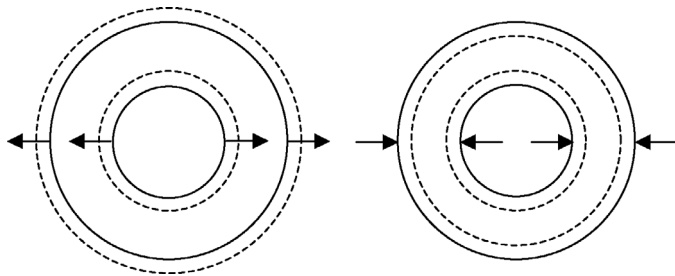


Fig. 1. Displacement loci of (a) radial and (b) wall-thickness mode of a ring. — Shape at rest, - - - deformed shape.

## II. VIBRATION CHARACTERISTICS OF PZT RINGS

To understand the working principle of the proposed PT, it should start with the resonance characteristics of a PZT ring. For a fully electroded PZT ring, several main resonances would be identified in the frequency domain. It includes the radial, wall-thickness, thickness, and other complex modes [8]. The radial and wall-thickness modes are also referred to as the first and second order extensional modes of a ring, respectively. The loci of the motions are shown in Fig. 1. The inner and outer walls move in phase in the first order extensional mode, and two walls move out-of-phase in the second order mode. However, extensional modes with higher order modes are often very weak or even vanished in the frequency spectrum. It is because radial tensile and compressive stresses cancel each other at the high-order modes. A 3-D finite-element analysis was performed to understand the phenomena. Consider the deformation and radial stress profile of the cross section of a ring at its extensional modes in Fig. 2. For mode order ( $m$ ) equals to 1 and 2, the radial stress distributions are of the same sign. The whole ring is under either radial compression or tension; hence, it results in a maximum net stress level. The high stress implies a strong coupling mode could be excited electrically. However, when  $m$  becomes larger, the radial stress profile contains a number of positive and negative regions. Therefore, the resultant stress level is reduced or even totally cancelled each other. Hence, only a very weak coupling can be identified in the electrical impedance spectrum. To excite the higher-order radial extensional modes of a PZT ring, the compressive and tensile stress regions have to be decoupled by splitting the electrode according to the stress distribution. For example, the third radial extensional mode could be excited by splitting the electrode at its nodal line of the radial stress as shown in Fig. 3. By driving the PZT ring at either the positive or negative stress region, the third order mode could be excited. Similarly, higher-order modes could be excited by using more concentric electrodes.

A commercial PZT ring, (Fuji 213, Fuji Ceramics Ltd., Shizuoka, Japan), with an outer diameter of 12.7 mm, inner diameter of 5.1 mm, and a thickness of 1.2 mm is used to demonstrate this idea. The PZT ring has silver electrodes on two main surfaces and is poled along its thickness direction. The materials properties provided by the

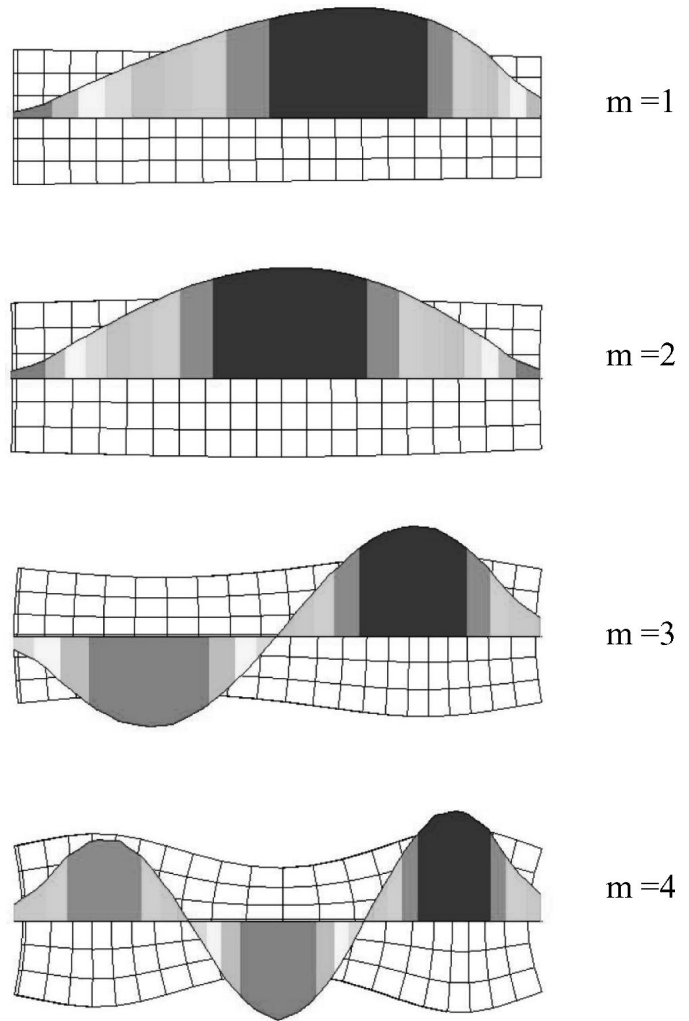


Fig. 2. Radial stress profiles of a cross-sectional deformation ring by FEM.

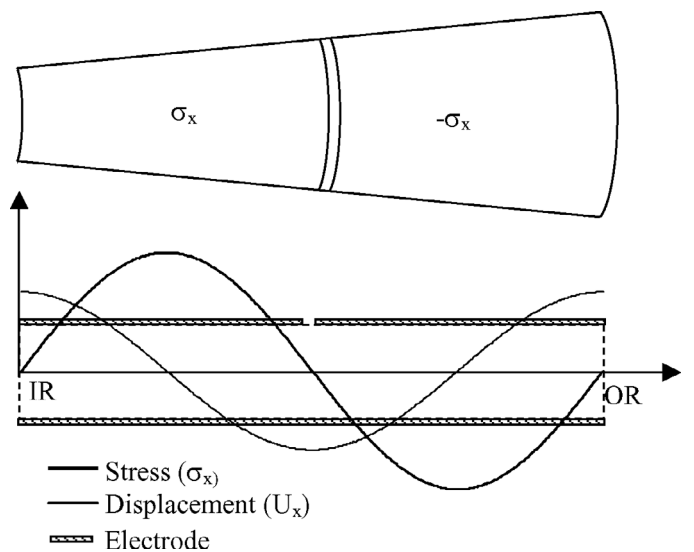


Fig. 3. Electrode configuration for the third radial extensional mode of a PZT ring.

TABLE I  
MATERIAL PROPERTIES OF PZT RING.

Elastic modulus	$E_{11}$ (GPa)	72
	$E_{33}$ (GPa)	6.0
Density	$\rho$ (kgm <sup>3</sup> )	7700
Poisson's ratio	$\sigma$	0.29
Permittivity	$\epsilon_{11}^T$	1450
Piezoelectric constant	$d_{33}$ (10 <sup>-12</sup> m/V)	330
	$d_{31}$ (10 <sup>-12</sup> m/V)	-145
Mechanical quality factor	$Q_m$	2000

supplier are listed in Table I. Two rings were designed to excite resonance modes with  $m$  equal to 3 and 4. One of the electrodes of the PZT ring is split into two concentric regions to excite the  $m = 3$  mode. Other PZT rings have three concentric electrodes in order to excite the fourth order mode. All the allowable modes of the two rings together with one full electrode sample were measured by a HP 4149A Impedance/Gain Phase Analyzer (Hewlett-Packard, Palo Alto, CA), and results are shown in Fig. 4. The measurement also was compared with the FEM prediction. Good agreement could be obtained. For Fig. 4(a), the fully electroded ring could excite two strong coupling modes at 120 kHz ( $m = 1$ ) and 453 kHz ( $m = 2$ ). With splitting the driving electrode into two concentric rings, the strongest coupling occurred at 818 kHz ( $m = 3$ ). Upon further splitting the electrode into three parts, the main resonance was shifted to 1073 kHz ( $m = 4$ ). The analytical approximation of the resonance frequencies of the extensional modes of a ring is given by [6]:

for  $m = 1$ ,

$$f_r = \frac{1}{2r_o} \sqrt{\frac{C_{11}^E}{\rho}}, \quad (1)$$

for  $m = 2$ ,

$$f_r = \frac{2}{\pi(r_o - r_i)} \sqrt{\frac{C_{11}^E}{\rho}}, \quad (2)$$

for  $m > 3$ ,

$$f_m = \frac{\alpha_m}{2\pi r_o} \sqrt{\frac{Y_{11}}{\rho(1 - \sigma^2)}}, \quad \alpha_m \approx \frac{m - 1}{1 - r_i/r_o} \pi, \quad (3)$$

where  $r_i$  and  $r_o$  are the inner and outer radius of the PZT ring, and  $C_{11}^E$ ,  $Y_{11}$ ,  $\rho$ , and  $\sigma$  are the stiffness, Young's modulus, density and Poisson's ratio of the PZT materials, respectively. The resonance frequencies found by analytical, finite-element simulation and measurement are listed in Table II.

In order to identify that the correct extensional modes of a ring are excited, a Polytec laser vibrometer (Physik Instruments, Inc., Karlsruhe, Germany) was used to scan the out-plane displacement on the major surface along the radial direction. The scanning path starts from the inner radius to the outer radius. The mode shapes predicted by

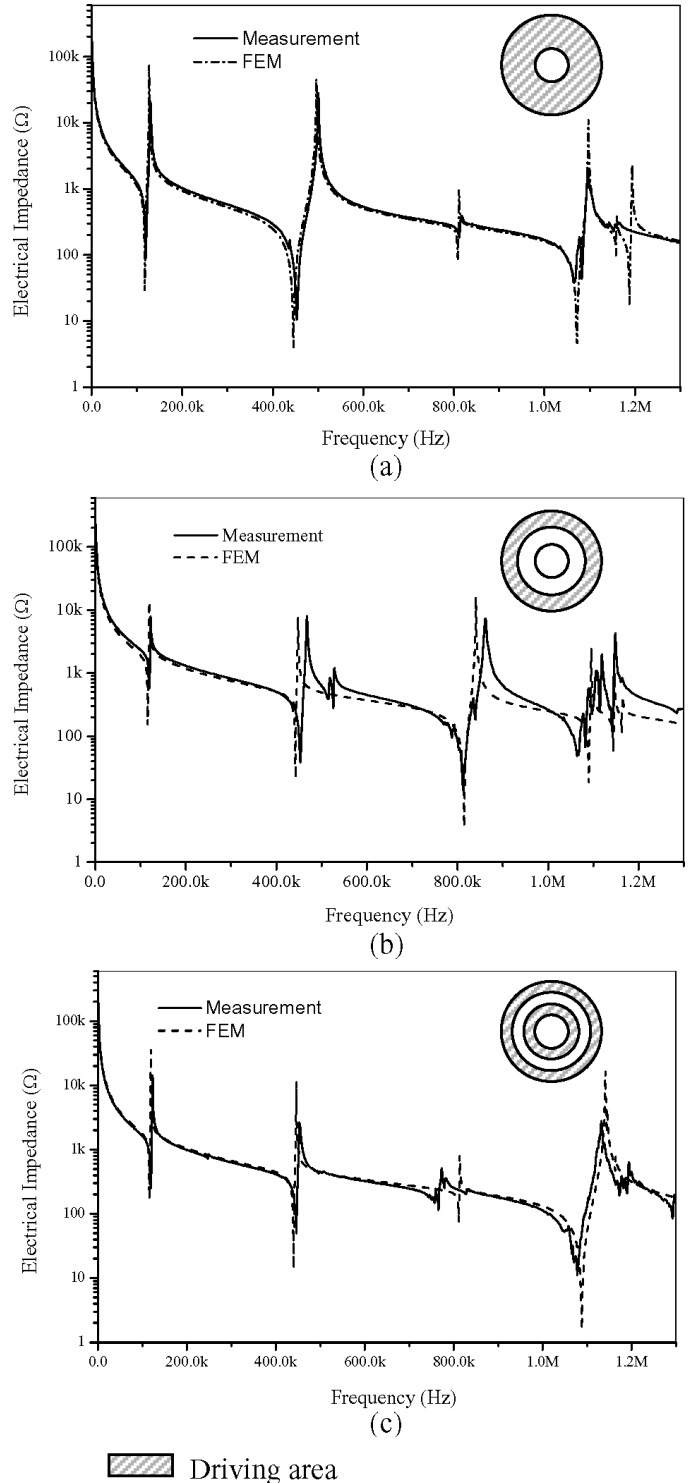


Fig. 4. Electrical impedance spectrum of a PZT ring at higher order modes excitation (a) Fully electroded ring. (b) Two concentric electrodes. (c) Three concentric electrodes.

TABLE II  
COMPARISON ON RESONANT FREQUENCIES OF PZT RING AT HIGHER  
ORDER EXTENSIONAL MODES.

Order	Analytical (kHz)	Experiment (kHz)	FEM (kHz)
$m = 1$	103.2	119.7	118.2
$m = 2$	463.5	453.3	446.8
$m = 3$	838.2	818.0	815.2
$m = 4$	1141.1	1073.0	1087.1

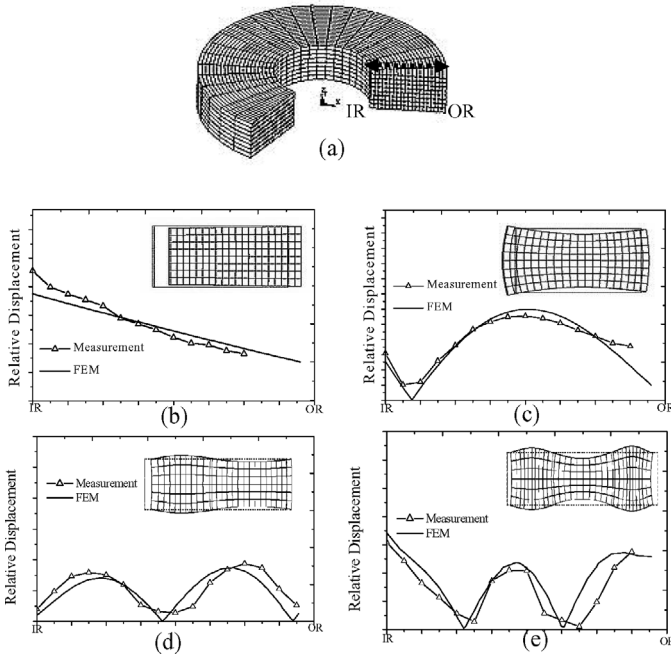


Fig. 5. Laser measurement results. (a) Laser scanning path. (b)–(e) Out-plane displacement profiles for  $m = 1$  to 4.

the FEM and found by laser measurement are plotted in Fig. 5. Fig. 5(a) shows a 3-D FEM with the scanning path of the laser measurement. The first and second order extensional modes excited by a full electrode ring are shown in Figs. 5(b) and (c). As the laser measurement cannot detect the direction of motion, the absolute displacement from FEM is plotted as comparison. The deformed shape of the cross section of a ring is used to illustrate the actual vibration profile of the ring. From Figs. 5(d) and (e), the vibration profiles for  $m = 3$  and 4 excited using concentric electrodes were plotted and compared with simulations. Again, good agreements were obtained from the FEM prediction and laser measurements. The results have experimentally verified that the higher-order extensional modes could be excited using the concentric electrode patterns.

### III. CONSTRUCTION AND OPERATION PRINCIPLE

The construction of the PT using higher-order extensional modes of a ring is to divide the top electrode into concentric regions. For example, to make use of the third order mode, two concentric electrodes have to be used.

And three concentric electrodes will be used for  $m = 4$ , and so on. According to the radial stress distribution, the compressive regions are connected together as the input section. Similarly, the tensile stress areas are connected as the output section. The bottom electrode served as a common ground for both input and output. The constructions of PTs using the third and fourth order modes are shown in Fig. 6. To minimize the disturbance on the resonance characteristics of the ring, the solder joints are applied at the displacement nodal lines as represented by the dotted lines in Fig. 6. The displacement nodal lines also can be used as the supporting positions for the PTs. The prototypes of a PT using third and fourth extensional modes are shown in Fig. 7. The characteristics of PTs are measured with an HP 4194A impedance gain/phase analyzer (Hewlett-Packard, Palo Alto, CA) and listed in Table III. The input characteristics were measured with the output section grounded. Similarly, the input section is grounded during the output characteristics measurements. The PT characteristics were measured under a free condition by placing the PTs on a soft foam. However, for practical applications, the PTs can be fixed either by mechanical clamping or solder joints at the displacement nodal lines.

From the characteristics of the PTs, it is obvious that the frequency of the PT changes as the order of mode number varies. In addition, when  $m$  increases from 3 to 4, apart from the frequency increases from 818 kHz to 1073 kHz, the matching load also reduces from 916  $\Omega$  to 360  $\Omega$ . Without changing the physical dimensions of the PT, the PT properties could be tailored design by using different mode order. It makes the ring PT most adaptable to various electronic devices. The higher order PTs also could provide ideal electromagnetic isolation in high-frequency circuits.

### IV. FINITE-ELEMENT ANALYSIS ON HIGHER-ORDER EXTENSIONAL MODES

Due to the size limitation, PT using fifth order or higher modes is difficult to fabricate. To study the characteristics of PTs using higher-order modes, a commercial finite-element code, ANSYS, was used as the computational tool. In past studies, the analysis of PTs were mostly based on the well-accepted equivalent circuit [10]. However, most of the equivalent circuits are derived from 1-D models or assumption, the vibration of the PT is actually on all three dimensions. At higher order modes, the activities of all the directions are comparable and should not be neglected. Therefore, the equivalent circuits may no longer be useful. The use of a 3-D FEM analysis is valuable in such cases. In ANSYS<sup>1</sup>, couple-field elements that can include both a mechanical and electrical degree of freedom (DOF) are used to construct the PT models. The element matrix is derived from the linear piezoelectric equations:

$$\begin{cases} \{T\} = [C]\{S\} - [e]\{E\} \\ \{D\} = [e]^T\{S\} + [\varepsilon]\{E\} \end{cases} \quad (4)$$

<sup>1</sup>ANSYS 5.6 Manual, ANSYS, Ltd.

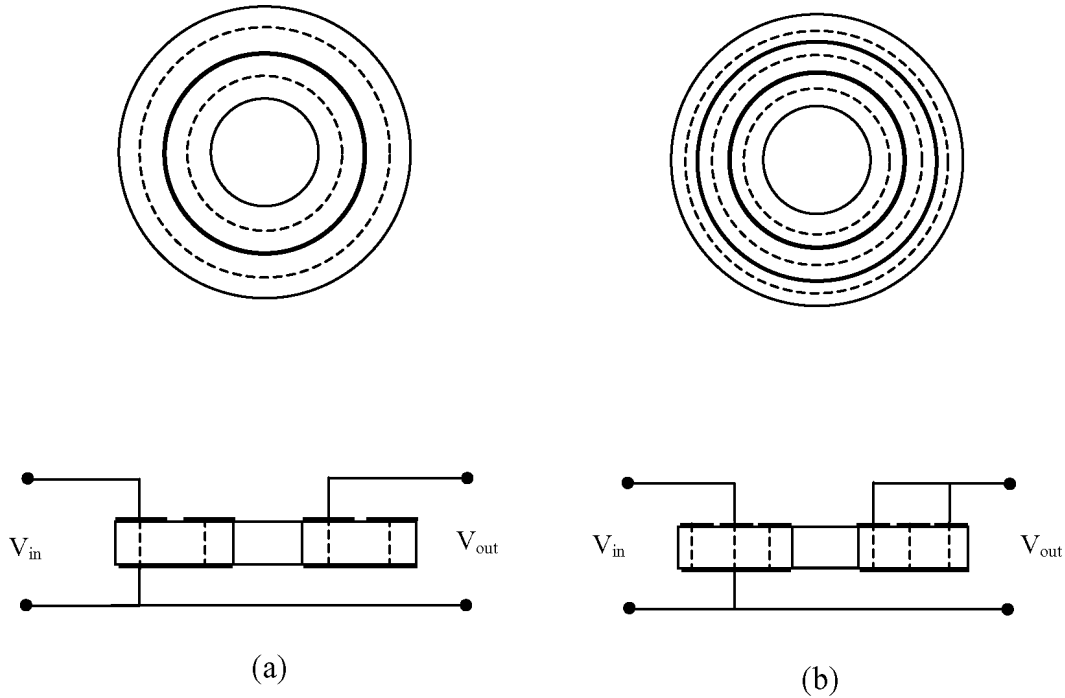


Fig. 6. Construction of piezoelectric transformer at (a) third and (b) fourth radial extensional mode.

where  $\{T\}$ ,  $\{S\}$ ,  $\{D\}$ , and  $\{E\}$  are the stress, strain, electric flux density and electric field vector, respectively.  $[C]$ ,  $[e]$ , and  $[\varepsilon]$  represent the elastic, piezoelectric, and dielectric matrix, respectively. By the variational principle and finite-element discretization, the coupled finite-element matrix equations can be derived. It can allow the element to take into account both direct and inverse piezoelectric effects at the same time in one model.

The 3-D FEM was constructed by 8-nodes brick couple field elements. The silver electrode was neglected in the model because it is much thinner than the thickness of the PZT ring. The equipotential boundary condition was applied to all the nodal points covered by a single electrode. It can simulate the physical conductive behaviors of the silver electrodes. Except for the geometry of PT, the characteristics also depended on the loading condition. The efficiency of PT will reach a maximum when the loading,  $R_L$ , is equal to  $1/(\omega C_{d2})$ , which is called the matching load of the PT [11]. However, the loading condition cannot be implemented into the present FEM. The open-circuit characteristics of PT will be investigated.

A PT uses the direct piezoelectric effect at the driver section to excite the whole structure in resonance. Electrical charges will be built up at the output section by the inverse piezoelectric effect. Hence, the performance of a PT will be determined by the effective electromechanical coupling factors at both input and output sections, represented by  $k_{in}$  and  $k_{out}$  hereafter. To evaluate the performance of a PT, the mean effective coupling factor will be used as a figure-of-merit, and it is given by:

$$k_m = \sqrt{k_{in} \times k_{out}}, \tag{5}$$

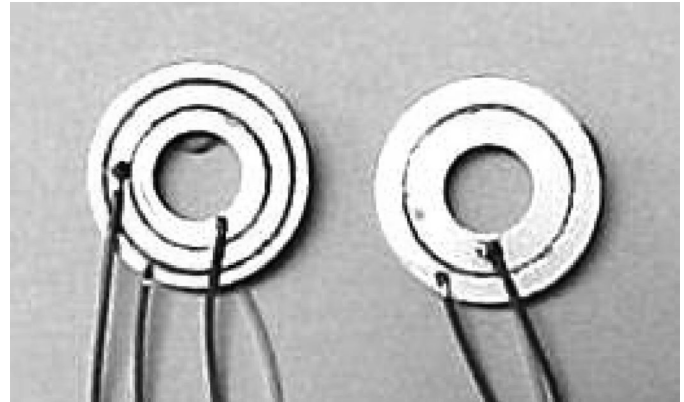


Fig. 7. Prototypes of piezoelectric ring transformers.

TABLE III  
CHARACTERISTICS OF PROTOTYPES.

	$m = 3$		$m = 4$	
	Input	Output	Input	Output
$F_r$ (kHz)	818.0	818.0	1073.0	1073.0
$F_a$ (kHz)	859.1	857.4	1127.6	1106.8
$R$ ( $\Omega$ )	9.4	16.0	15.3	81.4
$L$ (mH)	1.2	1.9	0.3	1.7
$C_a$ (pF)	33.2	19.8	68.5	13.2
$C_b$ (pF)	342.4	213.2	675.2	381.8
$Q_m$	626.3	616.4	141.6	137.5
$k_{eff}$	0.31	0.3	0.31	0.24

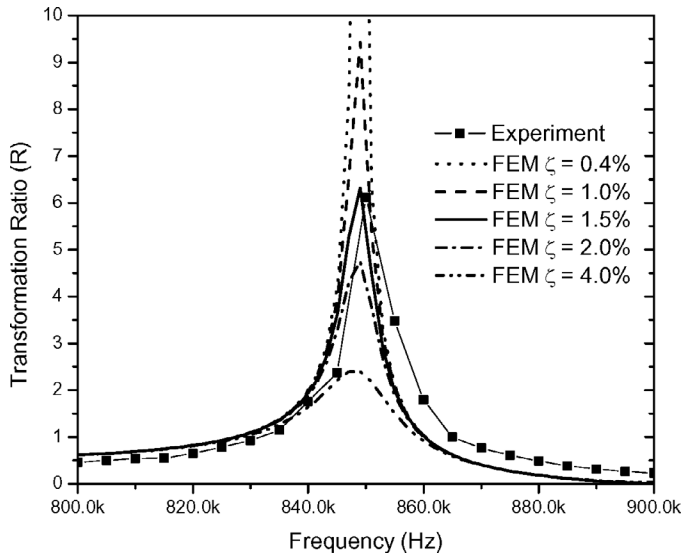


Fig. 8. Transformation ratio of the third order PT versus driving frequency under different damping ratios.

where  $k_{in}/k_{out} = \sqrt{(F_a^2 - F_r^2)/F_a^2}$ ,  $F_a$  and  $F_r$  are the resonance and antiresonance frequencies.

The input and output characteristics of  $F_r$  and  $F_a$  could be determined by a modal analysis of ANSYS. In a harmonic analysis, the open-circuit characteristics such as transformation ratio ( $R$ ) also could be predicted. However, the actual transformation ratio value will be determined by the loss factor of the PT. In this analysis, we have made an assumption that the damping ratio at a narrow frequency range, from 1 MHz to 2 MHz to be constant. The actual loss factor is found by fitting a constant damping ratio ( $\zeta$ ), which is defined as the percentage of critical damping, to match with the voltage response of a third order mode of the PT. The transformation ratio of a third order PT is compared with FEM simulation as shown in Fig. 8. It is found that  $R$  highly depended on the value of  $\zeta$ . By comparing different damping values,  $\zeta$  equal to 1.5% gives the best fitting with the experimental results. The PT could reach a maximum open-circuit transformation ratio of 6.2 at 851 kHz. A loss factor of 1.5% of critical damping will be used in all the FEM analysis.

The FEM prediction on the characteristics of PT using higher order modes (up to  $m = 7$ ) of a ring is shown in Fig. 9. The resonance frequencies of the PT increases as the mode order increases. It is also noticed that both  $k_m$  and  $R$  decrease at higher mode order. In the higher order modes, the wavelength decreases as the resonant frequency increases. The wavelength propagates in the radial direction and is comparable to the ring thickness. Hence, other complex modes in the thickness direction also could be excited simultaneously. Mode couplings will occur and reduce the  $k_m$  and  $R$  of the PT and the efficiency of the transformer. From the FEM results in Fig. 9,  $k_m$  of the PT reduced from 0.26 to 0.14 as  $m$  increases from 3 to 7. In addition,  $R$  also reduces from 6.2 to 3.2. To demonstrate the mode coupling in higher-order modes, the resonance

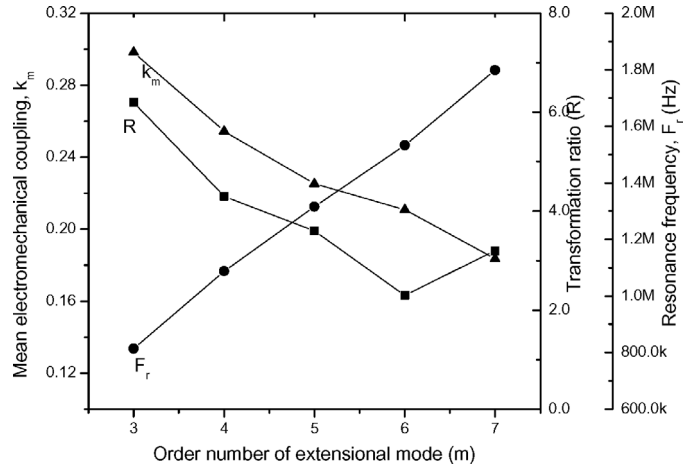


Fig. 9. Relationship among the mean electromechanical coupling factor, transformation ratio, resonant frequency with the order of modes.

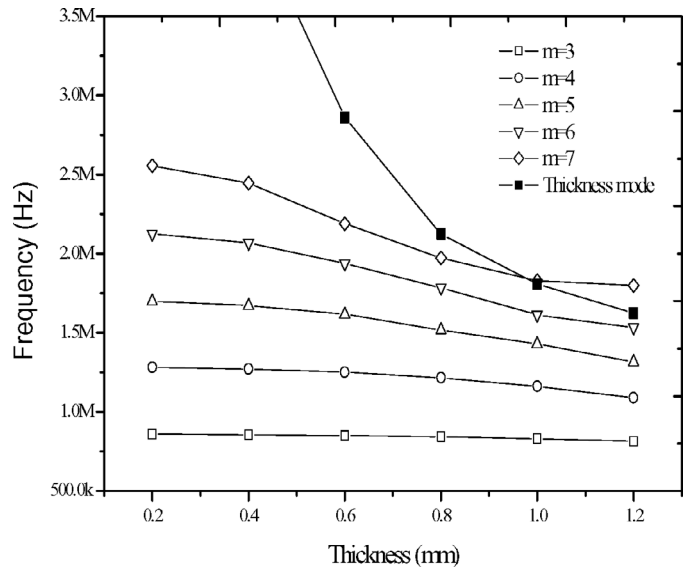


Fig. 10. Relationship of the resonant frequency with the ring thickness.

frequencies of the radial extensional modes and thickness mode are plotted against the ring thickness in Fig. 10. When the ring thickness varies from 0.8 to 1.2 mm, the thickness mode falls into the range of the operation frequencies of PT with mode orders 5 to 7. The mode coupling between thickness and radial modes could happen. When the ring thickness is less than 0.6 mm, mode coupling with thickness mode will no longer exist. The  $k_m$  of the PT in higher-order modes are shown in Fig. 11. In general,  $k_m$  decreases as the ring thickness increases. However, for a 0.8 to 1.2-mm thick ring,  $k_m$  drops significantly, and the trend also was distorted. It is the evidence of mode-coupling effect with the thickness mode that reduces  $k_m$  of the PT. As the thickness approaches to zero, the value of  $k_m$  will be similar at all mode orders. Therefore, when the ring thickness becomes very small, the performance of the PT will be independent of the mode order.

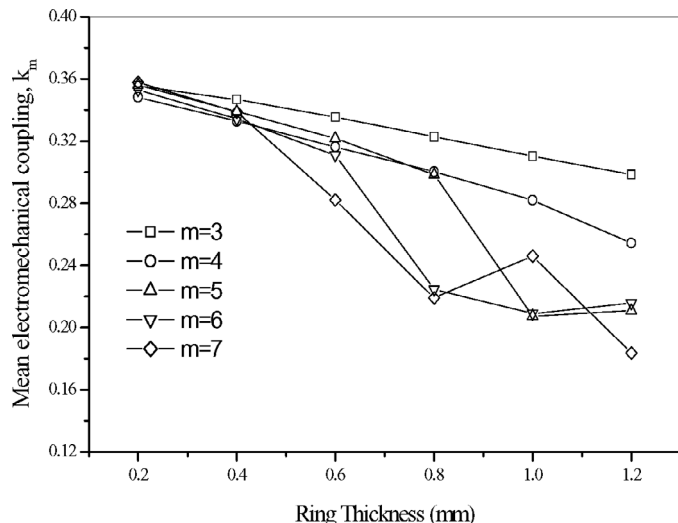


Fig. 11. Relationship of the mean electromechanical coupling factors with the ring thickness.

## V. CONCLUSIONS

The use of PZT ring as a transformer was studied. The PT was designed to operate at the extensional mode of a ring. With proper designed concentric electrodes, the higher-order extensional modes could be excited, and PTs using higher order modes could be fabricated. Prototypes of PT of mode numbers 3 and 4 were fabricated to prove the proposed idea. Three-dimensional FEM were used to predict the characteristics such as resonant frequencies, transformation ratio, and mean electromechanical coupling factor of PT using higher order modes. It was found that, for a PZT ring with outer and inner diameter of 13.5 and 5.1 mm, the ring thickness has to be less than or equal to 0.6 mm to avoid mode coupling with the thickness mode. It also was found that, when the ring thickness becomes very small, the mean coupling factor will no longer depend on the mode number. Hence, the proposed PT will be ideal for a very thin structure, such that the operating frequency can be tuned without affecting the performance significantly. This study helps to optimize the ring-shape transformers for practical applications.

## REFERENCES

- [1] C. A. Rosen, "Ceramic transformer and filters," in *Proc. Electr. Component Symp.*, 1956, pp. 205–211.
- [2] Y. Fuda, K. Kumasaka, M. Katsuna, H. Sato, and Y. Ino, "Piezoelectric transformer for cold cathode fluorescent inverter," *Jpn. J. Appl. Phys.*, vol. 36, pp. 3050–3052, 1997.
- [3] O. Ohnishi, H. Kishie, A. Iwamoto, Y. Sasaki, T. Zaitso, and T. Inoue, "Piezoelectric ceramic transformer operating in thickness extensional vibration mode for power supply," in *Proc. IEEE Ultrason. Symp.*, 1992, pp. 483–488.
- [4] W. Pajewski, P. Kielczynski, and M. Szalewski, "Resonant piezoelectric ring transformer," in *Proc. IEEE Ultrason. Symp.*, 1998, pp. 977–980.
- [5] B. Koc, S. Alkoy, and K. Uchino, "A circular piezoelectric transformer with crescent shape input electrodes," in *Proc. IEEE Ultrason. Symp.*, 1999, pp. 931–934.

- [6] J. H. Hu, H. L. Li, H. L. W. Chan, and C. L. Choy, "A ring-shaped piezoelectric transformer operating in the third symmetric extensional vibration mode," *Sens. Actuators A*, vol. 88, pp. 79–86, 2001.
- [7] P. Laoratankaul, A. V. Carazo, P. Bouchilloux, and K. Uchino, "Unipoled disc-type piezoelectric transformers," *Jpn. J. Appl. Phys.*, vol. 41, pp. 1446–1450, 2001.
- [8] H. L. Li, H. L. W. Chan, and C. L. Choy, "Vibration characteristics of piezoceramics rings," *Ferroelectrics*, vol. 263, pp. 211–216, 2001.
- [9] H. L. Li, J. H. Hu, H. L. W. Chan, and C. L. Choy, "Ring-shaped piezoelectric transformer having an inner and outer electrode," U.S. patent US6597084, Jul. 2003.
- [10] C. Y. Lin and F. C. Lee, "Design of a piezoelectric transformer converter and its matching networks," *Power Electron. Specialists Conf. Record*, pp. 607–612, 1994.
- [11] T. Hayasaka and S. Yoshikawa, *Acoustics Vibration Theory*. Tokyo: Maruzem, 1974, p. 124.



**Hing Leung Li** was born in Hong Kong in 1974. He received his B.Eng. and M.Phil. degrees in the Department of Mechanical Engineering from the Hong Kong University of Science and Technology, Hong Kong, China, in 1996 and 1998, respectively.

Mr. Li is currently a mechanical engineer in ASM Assembly Automation Ltd., Hong Kong, and a part-time Ph.D. student in the Applied Physics Department of the Hong Kong Polytechnic University, Hungghom, Kowloon, Hong Kong. His research

interests are on design and modeling of piezoelectric devices.



**Jun Hui Hu** was born in China in August 1965. He received B.S. and M.S. degrees in electrical engineering from Zhejiang University, Zhejiang, China, and the Ph.D. degree from Tokyo Institute of Technology, Tokyo, Japan, in 1986, 1989, and 1997, respectively. He was a research associate at the Department of Electrical Engineering, Zhejiang University from September 1989 to July 1991, and a research engineer at R&D Centre of Tokin Corporation, Tokyo, Japan, from November 1997 to February 1999. Since March 1999, he has

been a postdoctoral research fellow at the Centre for Smart Materials, Department of Applied Physics, the Hong Kong Polytechnic University, Hong Kong.

His present research field includes ultrasonic motors, piezoelectric transformers, transducers, and other elastic wave functional devices.

Dr. Hu won the Paper Prize from the Institute of Electronics, Information and Communication Engineers (Japan) in 1998. He is the author or co-author of 12 pending patents on piezoelectric transformers. He is a member of IEEE-UFFC and the Acoustic Society of Japan.



**Helen Lai Wah Chan** received B.Sc. and M.Phil. degrees in physics from the Chinese University of Hong Kong in 1970 and 1974, respectively and received the Ph.D. degree in physics from Macquarie University, Sydney, NSW, Australia, in 1987.

She worked as a research scientist in the National Measurement Laboratory of the Commonwealth Scientific and Industrial Research Organization (CSIRO) Division of Applied Physics, Sydney, NSW, Australia in 1987–1991 and was responsible for setting up

the Australian Standards for sensor and transducer calibration in medical ultrasound. She then worked as a senior acoustic engineer at GEC-Marconi Pty., Sydney, Australia, for a year on hydrophone arrays for underwater acoustics before she returned to Hong Kong in 1992. She is currently Chair Professor of Applied Physics at the Hong Kong Polytechnic University, Hunghom, Kowloon, Hong Kong. Prof. Chan has published two book chapters, over 250 journal papers, 70 conference papers, and eight patents (with seven patents under application) in the areas of smart materials and devices, ultrasonic transducers, and fiber-optic sensors.